Gravastar in the framework of braneworld gravity

Rikpratik Sengupta,[*] Shounak Ghosh,[†] and Saibal Ray[‡]
Department of Physics, Government College of Engineering and Ceramic Technology, Kolkata 700010, West Bengal, India

B. Mishra[§]
Department of Mathematics, Birla Institute of Technology and Science-Pilani, Hyderabad Campus, Hyderabad 500078, India

S. K. Tripathy[‖]
Department of Physics, Indira Gandhi Institute of Technology, Sarang, Dhenkanal 759146, Odisha, India

(Received 2 April 2020; accepted 26 June 2020; published 10 July 2020)

Gravastars have been considered as a serious alternative to black holes in the past couple of decades. Stable models of gravastar have been constructed in many of the alternate gravity models besides standard general relativity (GR). The Randall-Sundrum (RS) braneworld model has been a popular alternative to GR, especially in the cosmological and astrophysical context. Here, we consider a gravastar model in RS brane gravity. The mathematical solutions in different regions have been obtained with calculation of matching conditions. Various important physical parameters for the shell have been calculated and plotted to note their variation with radial distance. We also calculate and plot the surface redshift to provide a very cursory check on the stability of the gravastar within the purview of RS brane gravity.

DOI: 10.1103/PhysRevD.102.024037

I. INTRODUCTION

There are a lot of heated debates regarding the final state of a stellar collapse in astrophysics just like the initial state of the Universe in cosmology. Einstein's general relativity (GR) has been tested quite rigorously through observational results in both astrophysics and cosmology considering intermediate energy phenomena. However, in situations with extremely high energies, like the initial state of the Universe and the end state of the stellar gravitational collapse, due to the fact that huge amount of energy is confined in a microscopic volume, the energy density almost diverges leading GR to predict singularities as the field equations break down completely [1], leaving room for considering quantum effects to come into play to avoid the undesirable singularities. In the case of stellar collapse of end states, the consideration of quantum field effects in classical GR leads to many interesting additional features about the most popular end-state solutions of black holes (BHs), like emission of the Hawking radiation from the event horizon [2] (which may be thought of as the boundary of a BH), but it cannot remove the singularities in this particular solution of the Einstein's field equations (EFEs) [3]. The singularity that occurs at the Schwarzschild radius $R = 2GM$ ($c = 1$) is not a physical singularity as the curvature invariants remain finite here and the singularity can be removed by a coordinate transformation. However, the central singularity that occurs at $r = 0$ being a physical singularity is irremovable.

In 2001, Mazur and Mottola (MM) [4] came up with the idea of a gravitational condensate star or *gravastar* as an alternative to a black hole, which they further developed in 2004 [5]. Chapline *et al.* [6–8] by taking quantum effects into consideration proposed that the horizon may be considered as the critical surface of a gravitational phase transition with the interior balancing the gravitational collapse of the surface by holding an equation of state (EOS) of the form $p = -\rho$ [9], where the negative pressure leads to a repulsive effect. By considering the fact that there is a phase transition at the horizon, MM extended this idea to quantum fluctuations which dominate over the temporal and radial components of the energy-momentum tensor at the horizon and grow large enough to lead to an EOS of the form $p = \rho$. This type of EOS is on the verge of violating causality and leads the interior to develop a gravitational Bose-Einstein condensate (BEC). Thus, the critical surface is replaced by a shell of stiff fluid introduced first by

[*]rikpratik.sengupta@gmail.com
[†]shnkghosh122@gmail.com
[‡]saibal@associates.iucaa.in
[§]bivudutta@yahoo.com
[‖]tripathy_sunil@rediffmail.com

Zeldovich [10,11]. This third region is the exterior which is pressureless and has zero energy density.

The gravitational force is weaker than the other three natural forces—the strong and weak nuclear forces, and the electromagnetic force. This is known as the hierarchy problem in particle physics. In an attempt to solve this problem, Randall-Sundrum (RS) proposed their first braneworld model [12] (RS-1) consisting of a positive and a negative tension brane with the former brane representing our Universe. The $(3+1)$ branes are embedded in a higher dimensional bulk. Only the force of gravity has accessibility to the bulk, while the other three forces are confined to the brane, thus making gravity the weakest of the forces. The higher dimensional gravity is the actual gravity at its full strength and cannot be realized in the brane. Later, they proposed another model [13] (RS-2) by sending the negative tension brane off to infinity. In this model, at low-energy limit, the Newtonian gravity can be recovered.

The single brane RS-2 model has been used extensively to study cosmological as well as astrophysical problems. The modifications due to RS-2 brane gravity (BG) have been studied in the cosmological context [14–20], whereas the study on modifications due to BG in astrophysical context was initially confined mostly to the study of the exterior solutions [21–25]. However, in the interior where the gravitational collapse takes place, the brane corrections to GR should be more significant as higher energy is involved in the collapse process [26–30].

Even in the context of GR, tackling exact interior solutions for the spherically symmetric matter distributions is extremely difficult [31]. In the case of a braneworld, the field equations have nonlocality and nonclosure properties due to the presence of projected Weyl tensor term on the brane [32], which makes it even more difficult to obtain exact interior solutions, only except uniform stellar-matter distributions, and can be thought of as an idealized situation. A better understanding of bulk geometry and brane-embedding properties is required for constructing exact interior solutions with a realistic nonuniform distribution which has been achieved through an elegant technique called the minimum geometric deformation approach developed by Ovalle in a series of papers [33–35]. The approach has also been applied successfully to obtain exact interior solutions for the nonuniform spherically symmetric matter distributions [36–38]. Apart from all these theoretical applications, a few experimental evidences in support of braneworld idea have been added in Refs. [39,40]. It has interestingly been shown there that the bulk geometry and brane embedding have applications in connection to the recent near-simultaneous detection of the gravitational-wave (GW) event GW170817 from the LIGO/Virgo Collaboration, and its electromagnetic counterpart, the short gamma-ray burst GRB170817A detected by the Fermi gamma-ray burst monitor, and the INTEGRAL anticoincidence shield spectrometer [39], and in the RS AdS_5 braneworld scenario the observation of M87*'s dark shadow can be explained [40].

In this paper, we consider a gravastar in an RS-2 braneworld model. Such a problem has been discussed by Banerjee *et al.* [41] but considering the conformal motion and freezing one of the metric potentials. However, we shall not consider conformal motion in our approach to obtain explicit solutions of the EFEs. Note that there is an effective cosmological constant on the brane but no charge has been considered in this work unlike Ghosh *et al.* [42], who considered the problem of a charged gravastar in higher dimensions.

The present investigation has been organized as follows: the field equations for the spherically symmetric metric on an RS-2 brane are provided in Sec. II along with explicit mathematical solutions to the field equations considering the EOS for the interior, shell, and exterior of the gravastar. However, in Sec. III, we study various physical parameters of the gravastar. In Sec. IV, the boundary conditions are computed which is followed by discussion and conclusion of the results in Sec. V.

II. MATHEMATICAL FORMALISM AND SOLUTIONS

A. Field equations on the brane

The EFE on the RS-2 with three-brane has the form

$$G_{\mu\nu} = T_{\mu\nu} + \frac{6}{\sigma} S_{\mu\nu} - E_{\mu\nu}, \tag{1}$$

where σ is the brane tension. Here we have used the geometrical units, $8\pi G = c = 1$.

The second and third terms on the rhs of the above equation represent the local and nonlocal corrections to GR due to the brane effects, respectively. The term $S_{\mu\nu}$ is quadratic in the energy momentum that arises due to the high-energy effects, and $E_{\mu\nu}$ represents the projected Weyl tensor on the brane which can be said to be the Kaluza-Klein correction. These terms can be expressed as follows:

$$S_{\mu\nu} = \frac{TT_{\mu\nu}}{12} - \frac{T_{\mu\alpha}T^{\alpha}_{\nu}}{4} + \frac{g_{\mu\nu}}{24}(3T_{\alpha\beta}T^{\alpha\beta} - T^2), \tag{2}$$

$$E_{\mu\nu} = -\frac{6}{\sigma}\left[Uu_\mu u_\nu + Pr_\mu r_\nu + h_{\mu\nu}\left(\frac{U-P}{3}\right)\right], \tag{3}$$

where T in Eq. (2) is the trace of the energy-momentum tensor.

The usual four dimensional (4D) energy-momentum tensor on the three-brane is given as

$$T_{\mu\nu} = \rho u_\mu u_\nu + p h_{\mu\nu}, \tag{4}$$

where $h_{\mu\nu} = g_{\mu\nu} + u_\mu u_\nu$ is the projected metric on the brane, u_μ denotes four-velocity, r_μ denotes the projected

radial vector, ρ and p, respectively, denote the energy density and pressure of the matter distribution, U and P denote the bulk energy density and bulk pressure, respectively. The last two quantities are taken to be related by the bulk EOS $P = \omega U$ [43], where ω is the EOS parameter that lies between $-3 < \omega < 2$. Here, we consider the relationship between the energy densities of the brane (ρ) and the bulk (U) by $U = A\rho + B$ [44], where A and B are constants which can be determined from the boundary conditions whereas ω is to be fixed on certain physical basis.

The static spherically symmetric line element describing the matter distribution on the three-brane is given by

$$ds^2 = -e^{\nu(r)}dt^2 + e^{\lambda(r)}dr^2 + r^2(d\theta^2 + \sin^2\theta d\phi^2). \tag{5}$$

The EFE on the brane, given by Eq. (1), can be computed to be

$$e^{-\lambda}\left(\frac{\lambda'}{r} - \frac{1}{r^2}\right) + \frac{1}{r^2} = \rho^{\text{eff}}, \tag{6}$$

$$e^{-\lambda}\left(\frac{\nu'}{r} + \frac{1}{r^2}\right) - \frac{1}{r^2} = p_r^{\text{eff}}, \tag{7}$$

$$e^{-\lambda}\left(\frac{\nu''}{2} - \frac{\lambda'\nu'}{4} + \frac{\nu'^2}{4} + \frac{\nu' - \lambda'}{2r}\right) = p_t^{\text{eff}}, \tag{8}$$

where

$$\rho^{\text{eff}} = \rho(r)\left(1 + \frac{\rho(r)}{2\sigma}\right) + \frac{6U}{\sigma},$$

$$p_r^{\text{eff}} = p(r) + \frac{\rho(r)(p(r) + \frac{\rho(r)}{2})}{\sigma} + \frac{2U}{\sigma} + \frac{4P}{\sigma},$$

$$p_t^{\text{eff}} = p(r) + \frac{\rho(r)(p(r) + \frac{\rho(r)}{2})}{\sigma} + \frac{2U}{\sigma} - \frac{2P}{\sigma}.$$

As evident from Eqs. (7) and (8), the pressure is not the same in the radial and transverse directions and hence there is a pressure anisotropy amounting to $6P/\sigma$. The effective pressure on the brane in the radial and angular directions is different due to the difference in contribution from the term containing the bulk pressure. This difference in the two pressure components of the energy-momentum tensor gives rise to the pressure anisotropy for effective matter distribution on the brane. This automatically justifies the claim by Cattoen [45] that gravastars must have anisotropic pressures, without forcing any anisotropy *a priori* by hand. This is an essential intrinsic feature of the braneworld gravastar which is absent within the framework of GR. On the other hand, from the physical point of view, the above expression ρ^{eff} defines the effective density on the brane, which includes the local and nonlocal corrections to the brane energy density ρ. The corrections are computed by evaluating the $00(tt)$ component of Eqs. (2) and (3), respectively. In this connection, we would like to mention that Maartens [46] has argued that the nonlocal bulk effects can contribute to effective imperfect fluid terms even when the matter on the brane has perfect fluid form. There is, in general, an effective momentum density and anisotropic stress induced on the brane by massive Weyl modes of the 5D graviton.

However, the conservation equation, i.e. Tolman-Oppenheimer-Volkoff (TOV) equation, on the brane reads the same as in GR,

$$\frac{dp}{dr} = -\frac{1}{2}\frac{d\nu}{dr}(p + \rho). \tag{9}$$

B. Interior solution

It is already mentioned that the interior of the gravastar has an EOS of the form $p = -\rho$. Such an EOS is responsible for a force to be created in the interior, which is now a gravitational BEC after the phase transition occurs at the horizon (replaced by a shell for a gravastar) and acts along the radially outward direction to oppose the collapse to continue. Plugging this EOS in the conservation equation (9), we get that $p = -\rho = -\rho_c$, where ρ_c is the constant interior density, thus implying constant pressure. In order to compute the metric potentials, we need to replace the pressure and energy density on rhs of Eqs. (6) and (7) by the pressure and energy density of the interior, respectively. This gives us the field equations in the following forms:

$$e^{-\lambda}\left(\frac{\lambda'}{r} - \frac{1}{r^2}\right) + \frac{1}{r^2} = \rho_c\left(1 + \frac{\rho_c}{2\sigma}\right) + \frac{6}{\sigma}(A\rho_c + B), \tag{10}$$

$$e^{-\lambda}\left(\frac{1}{r^2} + \frac{\nu'}{r}\right) - \frac{1}{r^2} = -\rho_c\left(1 + \frac{\rho_c}{2\sigma}\right) + \frac{2}{\sigma}(A\rho_c + B) + \frac{4\omega}{\sigma}(A\rho_c + B). \tag{11}$$

From Eq. (10), the first metric potential can be computed to be

$$e^{-\lambda} = 1 - \left[\frac{\rho_c}{3}\left(\frac{2\sigma + \rho_c}{2\sigma}\right) + \frac{2(A\rho_c + B)}{\sigma}\right]r^2 + \frac{c_1}{r}. \tag{12}$$

To make the solution regular at the origin, one can demand for $c_1 = 0$ and so we are left with

$$e^{-\lambda} = 1 - \left[\frac{\rho_c}{3}\left(\frac{2\sigma + \rho_c}{2\sigma}\right) + \frac{2(A\rho_c + B)}{\sigma}\right]r^2. \tag{13}$$

Now, using Eqs. (13) and (7), the second metric potential is given by

$$e^{-\nu} = C\left\{\left(\rho_c\left(1+\frac{\rho_c}{2\sigma}\right)+6\frac{A\rho_c+B}{\sigma}\right)r^2-3\right\}^{\left[1+\frac{\frac{6(A\rho_c+B)(1+2\omega)}{\sigma}-3\rho_c(1+\frac{\rho_c}{2\sigma})}{\rho_c(1+\frac{\rho_c}{2\sigma})+\frac{6(A\rho_c+B)}{\sigma}}\right]}, \tag{14}$$

where C is an integration constant.

From the above solutions, it can be noticed that the interior solutions have no singularity and thus the problem of the central singularity of a classical black hole can be averted.

C. Active gravitational mass $M(R)$

One can calculate the active gravitational mass for the interior of the gravastar as follows:

$$\begin{aligned} M(R) &= 4\pi\int_0^R \rho^{\text{eff}} r^2 dr \\ &= \frac{4\pi}{3}\left[\rho_c\left(1+\frac{\rho_c}{2\sigma}\right)+\frac{6}{\sigma}(A\rho_c+B)\right]R^3. \end{aligned} \tag{15}$$

It is to be noted that the active gravitational mass also depends on the brane tension σ.

D. Intermediate thin shell

The intermediate thin shell is a junction formed between the interior and exterior spacetimes. The shell is extremely thin but has a finite thickness. So, one can consider the condition $e^{-\lambda} \ll 1$ as suggested by Mazur and Mottola [4,5]. The field equations for the shell with EOS $p = \rho$ describing stiff fluid cannot be solved analytically until we take the approximation $e^{-\lambda} \ll 1$. On taking this approximation, it turns out that the equations can be solved easily and on integrating we obtain the expression for the metric potential such that it is proportional to the thickness of the shell ϵ. So, $e^{-\lambda} \ll 1$ implies $\epsilon \ll 1$, i.e., it is equivalent to considering a thin shell. Hence, it is called thin-shell approximation. It has been observed that the field equations (6)–(8) can be solved numerically only with the EOS $p = \rho$ in the shell. However, there is a possibility to obtain a set of analytic solutions of the metric functions of the shell considering the thin shell limit which demands this restriction. This facilitates to explore various properties of the thin shell. Under this thin shell approximation, the field equations (6)–(8) are modified as

$$\frac{e^{-\lambda}\lambda'}{r}+\frac{1}{r^2} = \rho\left(1+\frac{6A}{\sigma}\right)+\frac{\rho^2}{2\sigma}+\frac{6B}{\sigma}, \tag{16}$$

$$-\frac{1}{r^2} = \rho\left\{1+\left(\frac{1+2\omega}{\sigma}\right)2A\right\}+\frac{3\rho^2}{2\sigma}+\left(\frac{1+2\omega}{\sigma}\right)2B, \tag{17}$$

$$-\frac{\lambda'\nu'}{4}e^{-\lambda}-\frac{e^{-\lambda}\lambda'}{2r} = \rho\left\{1+\left(\frac{1-\omega}{\sigma}\right)2A\right\}+\frac{3\rho^2}{2\sigma}+\left(\frac{1-\omega}{\sigma}\right)2B. \tag{18}$$

The shell is composed of the Zel'dovich stiff fluid with the EOS in the form $p = \rho$. Putting this EOS in the conservation equation on the brane, i.e., Eq. (9), we obtain a relation between the metric potential ν and energy density of the shell ρ as

$$\rho = \rho_0 e^{-\nu}, \tag{19}$$

where ρ_0 is a constant of integration.

Equation (17) is a quadratic equation for ρ, considering the positive root of which we get the metric potential as

$$e^{-\nu} = -\frac{J}{6G\rho_0}+\sqrt{\frac{J^2}{36G^2\rho_0^2}-\frac{H_2}{36\rho_0^2}-\frac{1}{3G\rho_0^2 r^2}}. \tag{20}$$

The field equations (16) and (18) can be solved to obtain

$$\begin{aligned} e^{-\lambda} = {} & \frac{4\ln r}{3}+\left(\frac{J}{36}-\frac{F}{12}\right)\frac{r}{G}\sqrt{(J^2-12GH_2)r^2-12G} \\ & +\left(\frac{FJ}{12G}-\frac{H_1}{2}+\frac{H_2}{6}-\frac{J^2}{36G}\right)r^2 \\ & +\frac{(F-\frac{J}{3})}{\sqrt{12GH_2-J^2}}\arctan\left[\frac{(\sqrt{12GH_2-J^2})r}{\sqrt{(J^2-12GH_2)r^2-12G}}\right], \end{aligned} \tag{21}$$

where $F = 1+\frac{6A}{\sigma}$, $G = \frac{1}{2\sigma}$, $H_1 = \frac{6B}{\sigma}$, $H_2 = 2B(\frac{1+2\omega}{\sigma})$, $J = 1+2A(\frac{1+2\omega}{\sigma})$, $K = 1+2A(\frac{1-\omega}{\sigma})$ and $H_3 = 2B(\frac{1-\omega}{\sigma})$.

E. Exterior region

The exterior of the gravastar is assumed to obey the EOS, $p = \rho = 0$, which means that the outside region of the shell is completely vacuum. In this case, Eq. (6) reduces to

$$e^{-\lambda}\left(\frac{\lambda'}{r}-\frac{1}{r^2}\right)+\frac{1}{r^2} = \frac{6B}{\sigma}. \tag{22}$$

The solution has the form

$$e^{-\lambda} = 1-\frac{2M}{r}-\frac{2B}{\sigma}r^2, \tag{23}$$

where M is integration constant.

This can be compared with a de Sitter solution in $(3+1)$ dimension, and the corresponding line element can be written as

$$ds^2 = -\left(1-\frac{2M}{r}-\frac{\Lambda r^2}{3}\right)dt^2 + \left(1-\frac{2M}{r}-\frac{\Lambda r^2}{3}\right)^{-1}dr^2 + r^2(d\theta^2+\sin^2\theta d\phi^2). \quad (24)$$

Here the integration constant M gives the total mass of the gravastar, and Λ is the effective brane cosmological constant given by $\Lambda = \frac{6B}{\sigma}$. Since we consider the vacuum exterior, it can be argued from the RS model [13] that the effective cosmological constant on the brane vanishes as a consequence of the fine-tuning between the brane tension and the bulk cosmological constant. So, we claim $B=0=\Lambda$ for the vacuum exterior. Thus, as expected to be observed locally, the exterior solution reduces to the Schwarzschild solution

$$ds^2 = -\left(1-\frac{2M}{r}\right)dt^2 + \left(1-\frac{2M}{r}\right)^{-1}dr^2 + r^2(d\theta^2+\sin^2\theta d\phi^2). \quad (25)$$

F. Matching condition

In order to get the unknown constants, we adopted the matching condition of the metric functions at the junctions: (i) interior and shell ($r=R_1$) and (ii) shell and exterior ($r=R_2$). Now, one can match g_{tt} and $\frac{\delta g_{tt}}{\delta r}$ at $r=R_2$ to obtain the values of different constants, viz. $A=-504.9521017$, $B=3.01787$ inside the shell. In order to study different features of gravastar, we took the ratio of the matter densities of the shell and that of the core as $10^4(=\frac{\rho_0}{\rho_c})$, $\sigma = 10^3$ MeV/fm^3 and $\omega = 10^{-3}$. We also considered the following numerical values: $M = 3.75\ M_\odot$, $R_1 = 10$ km, and $R_2 = 10.1$ km.

III. PHYSICAL PARAMETERS OF THE MODEL

In this section, we shall be discussing some of the important physical parameters of the shell of the gravastar.

A. Pressure and matter density

It has been considered that the shell is formed with ultrarelativistic matter of extremely high density. The EOS has been stated as $p=\rho$. Using Eq. (17), we get the pressure as well as the matter density as follows:

$$\rho = p = \frac{\left(\sqrt{64r^2\left(\frac{\sigma^2}{16}+\frac{(A\sigma-3B)Y}{4}+\frac{A^2}{4}Y^2\right)\pi - 3\pi\sigma} + (-4YA-2\sigma)\pi r\right)}{6\pi r}, \quad (26)$$

where $Y = 2\omega+1$.

The variation of the energy density which is the same as the pressure of the shell along with the radial distance r is plotted in Fig. 1.

B. Energy

The energy of the shell is obtained as

$$E = 4\pi\int_R^{R+\epsilon}\rho^{\text{eff}}r^2dr = \frac{2}{3}\left[\frac{(4\pi r^2X-3\sigma+16A^2\pi r^2Y^2)^{3/2}}{12\pi^{\frac{1}{2}}(X+4A^2Y^2)} - \frac{\pi r^3}{3}(4AY+2\sigma)\right]_R^{R+\epsilon}, \quad (27)$$

where $X = (\sigma^2+8A\omega\sigma+4A\sigma-24B\omega-12B)$.

The variation of the energy of the shell along with the radial distance r is plotted in Fig. 2.

C. Entropy

The entropy is one of the most important parameters associated with a black hole. So, we must compute the

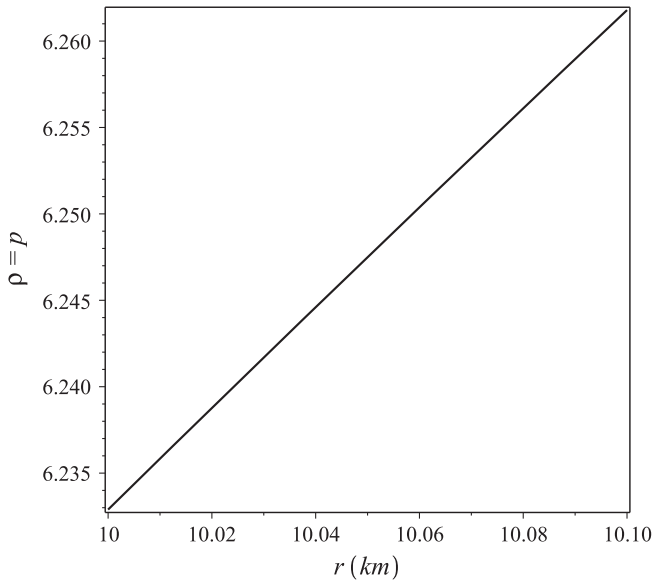

FIG. 1. Variation of the pressure or the matter density of the shell with respect to r.

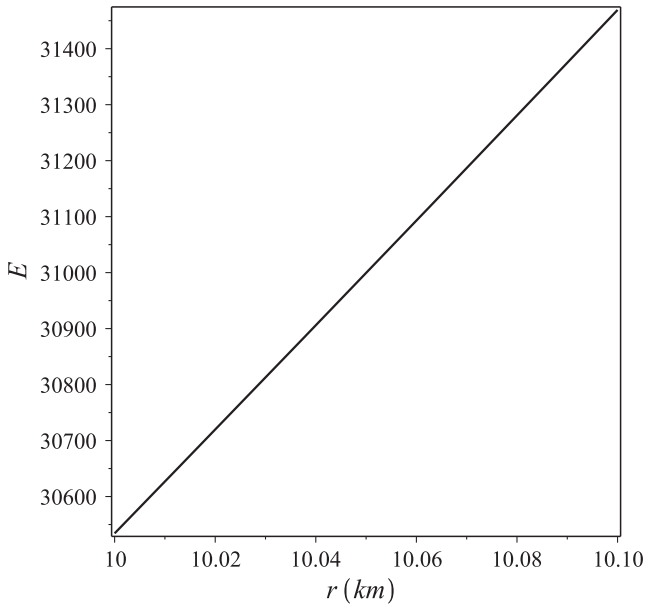

FIG. 2. Variation of the energy of the shell with respect to r.

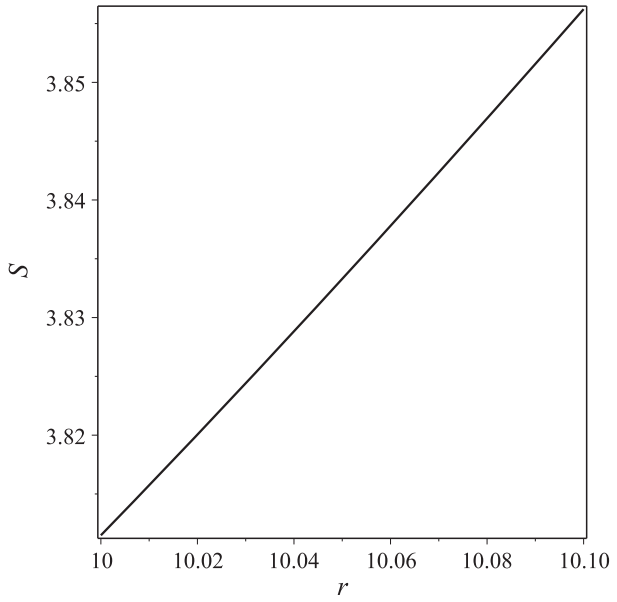

FIG. 3. Variation of the entropy (S) of the shell with respect to r (km).

entropy for a gravastar too. The entropy of the gravastar on the brane can be calculated using the following equation:

$$S = \int_R^{R+\epsilon} 4\pi r^2 s(r)\sqrt{e^{\lambda}}dr. \tag{28}$$

Here, $s(r)$ is defined as the entropy density and can be written as

$$s(r) = \frac{\xi^2 k_B^2 T(r)}{4\pi\hbar^2} = \frac{\xi k_B}{\hbar}\sqrt{\frac{p}{2\pi}}, \tag{29}$$

where ξ is a dimensionless constant. Considering the geometrical units (i.e., $G = 1$, $c = 1$) and also in the Planck units $k_B = 1$, $\hbar = 1$, Eq. (29) yields the following relation:

$$s(r) = \xi\sqrt{\frac{p}{2\pi}}. \tag{30}$$

Therefore, the entropy of the shell is obtained as

$$S = 4\pi\xi\int_R^{R+\epsilon} r^2\sqrt{\frac{pe^{\lambda}}{2\pi}}dr = \frac{4\pi\epsilon\xi R^2}{\sqrt{2\pi}}\left[\frac{4\ln R}{3} + \left(\frac{J}{36} - \frac{F}{12}\right)\frac{R}{G}\sqrt{(J^2 - 12GH_2)R^2 - 12G} + \left(\frac{FJ}{12G} - \frac{H_1}{2} + \frac{H_2}{6} - \frac{J^2}{36G}\right)R^2 + \frac{(F - \frac{J}{3})}{\sqrt{12GH_2 - J^2}}\arctan\left\{\frac{(\sqrt{12GH_2 - J^2})R}{\sqrt{(J^2 - 12GH_2)R^2 - 12G}}\right\}\right]^{-\frac{1}{2}} \times \sqrt{\frac{(\sqrt{64r^2(\frac{\sigma^2}{16} + \frac{(A\sigma - 3B)Y}{4} + \frac{A^2}{4}Y^2)\pi - 3\sigma\pi} + (-4YA - 2\sigma)R\pi)}{6\pi R}}. \tag{31}$$

The variation of entropy of the shell along with the radial distance r has been plotted in Fig. 3.

D. Proper thickness

The shell is considered to be extremely thin so that the phase boundaries are taken to be at R and $R + \epsilon$, where $\epsilon \ll 1$, such that the phase boundary of the interior essentially is at R. Therefore, the proper thickness of the shell is computed to be

$$\ell = \int_R^{R+\epsilon}\sqrt{e^{\lambda}}dr = \epsilon\sqrt{e^{\lambda}} = \epsilon\left[\frac{4\ln r}{3} + \left(\frac{J}{36} - \frac{F}{12}\right)\frac{r}{G}\sqrt{(J^2 - 12GH_2)r^2 - 12G} + \left(\frac{FJ}{12G} - \frac{H_1}{2} + \frac{H_2}{6} - \frac{J^2}{36G}\right)r^2 + \frac{(F - \frac{J}{3})}{\sqrt{12GH_2 - J^2}}\arctan\left\{\frac{(\sqrt{12GH_2 - J^2})r}{\sqrt{(J^2 - 12GH_2)r^2 - 12G}}\right\}\right]^{-\frac{1}{2}}. \tag{32}$$

E. Surface redshift

We compute the surface redshift in order to check the stability of our gravastar model. This is given by

$$Z_s = -1 + \frac{1}{\sqrt{g_{tt}}} = -1 + \sqrt{\frac{1}{6\rho_0\pi r}\left(8\sqrt{\left(r^2\left(\frac{\sigma^2}{16}+\frac{1}{2}(A\sigma-3B)X'+X'^2A^2\right)\pi-\frac{3\sigma}{64}\right)\pi}-2(4X'A+\sigma)r\pi\right)}, \tag{33}$$

where $X' = (\omega + \frac{1}{2})$.

We checked the variation of the surface redshift with respect to r in Fig. 4. It has been observed that without cosmological constant the surface redshift (Z_s) lies within the range $Z_s \leq 2$ [47–49]. However, Böhmer and Harko [49] argued that $Z_s \leq 5$ for the compact objects in the presence of cosmological constant. For our model, the surface redshift lies within 2 at every point of the shell.

IV. BOUNDARY CONDITION

The gravastar comprises the following three regions: (i) interior, (ii) shell, and (iii) exterior. The shell connects the interior to the exterior region at the junction interface. The metric coefficients are continuous across the interface, but the continuity of the first derivatives of the metric coefficients is not confirmed. The Darmois [50] and Israel [51] junction conditions allow us to compute the intrinsic surface stress energy at the junction in terms of the extrinsic curvature which connects the two sides of the thin shells geometrically. The intrinsic stress energy, following the prescription of Lanczos [52], turns out to have surface energy density and surface pressures as the temporal and spatial components, respectively. These components are computed to be of the form

$$\Sigma = -\frac{1}{4\pi R}\left[\sqrt{e^{\lambda}}\right]_-^+ = \frac{1}{4\pi R}\left[\sqrt{\left(1-\frac{2M}{R}\right)} - \sqrt{1-\left\{\frac{\rho_c}{3}\left(\frac{2\sigma+\rho_c}{2\sigma}\right)+\frac{2(A\rho_c+B)}{\sigma}\right\}R^2}\right], \tag{34}$$

$$\mathcal{P} = \frac{1}{16\pi}\left[\left(\frac{2-\lambda' R}{R}\right)\sqrt{e^{-\lambda}}\right]_-^+ = \frac{1}{8\pi R}\left[\frac{1-\frac{M}{R}}{\sqrt{1-\frac{2M}{R}}} - \frac{1-2\{\frac{\rho_c}{3}(\frac{2\sigma+\rho_c}{2\sigma})+\frac{2(A\rho_c+B)}{\sigma}\}R^2}{\sqrt{1-\{\frac{\rho_c}{3}(\frac{2\sigma+\rho_c}{2\sigma})+\frac{2(A\rho_c+B)}{\sigma}\}R^2}}\right]. \tag{35}$$

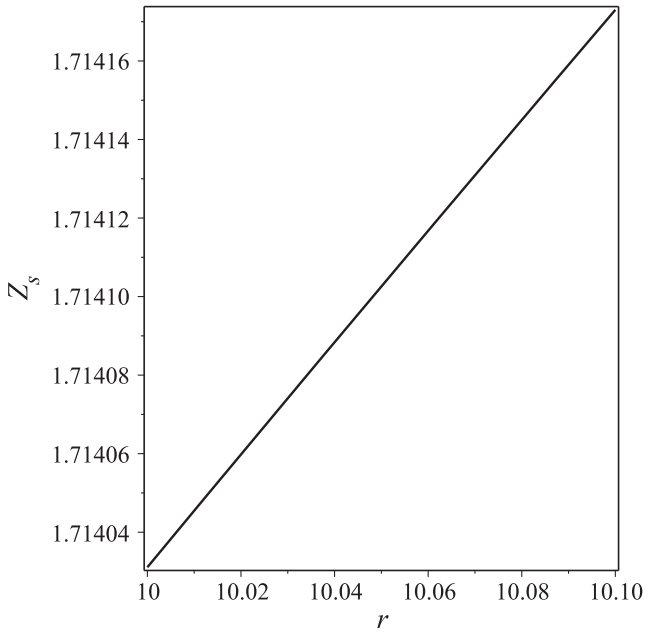

FIG. 4. Variation of the surface redshift of the shell with respect to r (km).

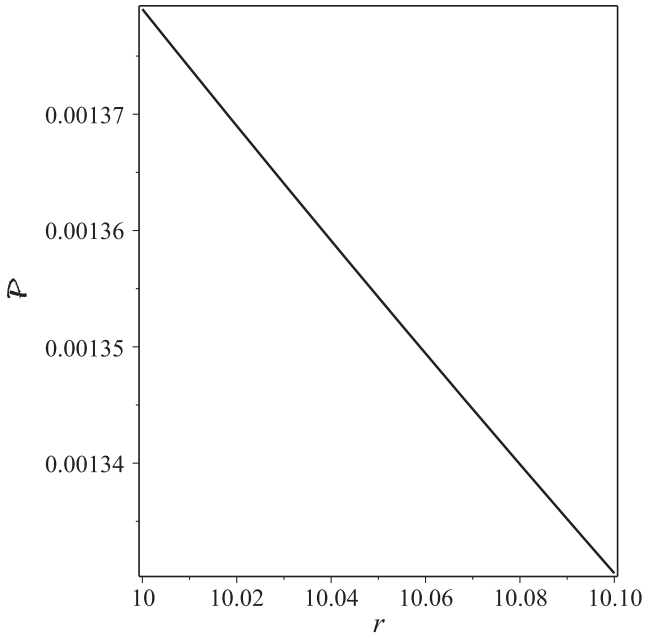

FIG. 5. Variation of the surface pressure of the shell with respect to r (km).

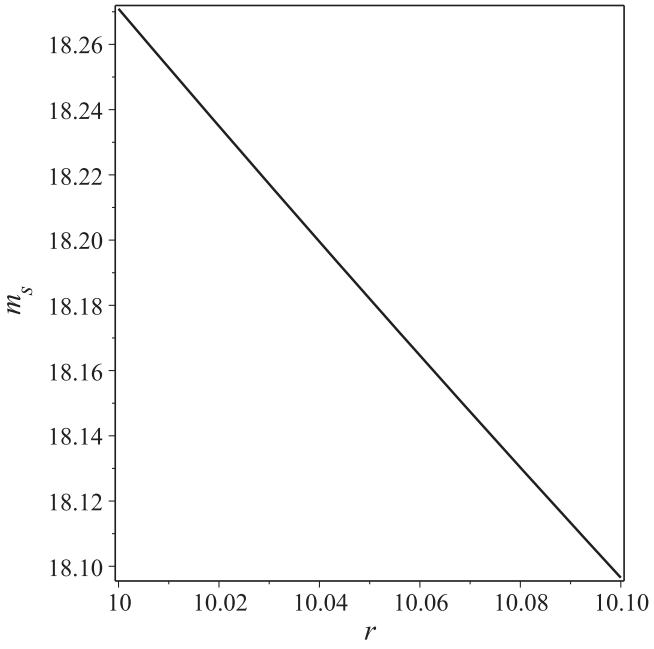

FIG. 6. Variation of the surface mass of the shell with respect to r (km).

The variation of the surface pressure of the shell is shown in Fig. 5. It is already mentioned that according to Mazur and Mottola [4,5] the thickness of the shell of the gravastar is very small but finite. In order to check the continuity between the interior and exterior spacetimes, we have studied here the Darmois [50] and Isreal [51] condition and calculated $\mathcal{P}$. So, here we have plotted $\mathcal{P}$ with respect to r to check the continuity. It is interesting to note that the surface pressure remains positive within the shell which justifies the EOS of the shell.

Now, the mass of the thin shell [using Eq. (34)] can be written as

$$\begin{aligned} m_s &= \int_R^{R+\epsilon} 4\pi R^2 \Sigma dr \\ &= \left[-\frac{1}{2}(M^2 \ln(R - M + \sqrt{(R-2M)R}) \right. \\ &\quad + \sqrt{(R-2M)R}(M-R)) \\ &\quad \left. + \frac{(36\sigma - 6R^2(12A\rho_c + 2\sigma\rho_c + {\rho_c}^2 + 12B))^{\frac{3}{2}}}{108\sqrt{\sigma}(12A\rho_c + 2\sigma\rho_c + {\rho_c}^2 + 12B)} \right]_R^{R+\epsilon}. \end{aligned} \tag{36}$$

We have plotted the variation of mass of the thin shell in Fig. 6.

V. DISCUSSIONS AND CONCLUSION

In this work, we studied gravastar in the framework of RS-2 brane gravity. The study of this model of gravitation was found to be interesting not only in the context that it modifies the EFE but also that the higher dimensions were involved. Following the earlier work done on gravastar under the modified theory of gravity models [53–56], a detail study was done on the three different regions of gravastar under braneworld theory.

Let us summarize some of the important physical properties of our study as follows:

(1) Interior region: By solving the TOV equation along with the EOS of the interior, it was found that the matter density and the pressure remain constant in the interior and the solution is free from singularity. We also calculated the active gravitational mass of the interior and it was observed that it has an additional dependence on the brane tension.

(2) Intermediate thin shell: To solve the intermediate thin shell, we applied the thin shell approximation and computed metric functions of it. The metric functions were found to be modified due to the braneworld effects reflected in the dependence on the brane tension and the bulk EOS parameter.

(3) Physical parameters of the shell: Various physical parameters associated with the shell were computed and the behavior was found to be modified due to the brane effects—both local and nonlocal. The details are provided as follows:
   (a) Matter density: We calculated the matter density and the pressure of the shell and plotted it against r as shown in Fig. 1. The variation of the matter density or pressure for the shell was found to be positive and constantly increased as we moved from the interior to the exterior surface.
   (b) Energy: The energy of the shell was obtained in Eq. (27), and the variation with respect to the radial parameter is shown in Fig. 2. The graph shows similar nature as the matter density of the shell, which suggests the physical acceptability of the model.
   (c) Proper length and entropy: We also calculated the entropy and the proper thickness of the shell and the solutions were found to be physically acceptable. The variation of the entropy with the radial parameter is plotted in Fig. 3 which displays a constantly increasing nature.
   (d) Surface energy density and surface pressure: Following the condition of Darmois and Israel [50,51], we calculated the surface energy density and the surface pressure and plotted the surface pressure against the radial parameter (Fig. 4). The surface pressure remained positive throughout the shell and decreased as we moved from the inner boundary of the shell to the outer which supports the formation and existence of the thin shell between the two spacetimes, i.e., interior and exterior.

(e) Surface redshift and surface mass: We checked the stability of the gravastar through a surface redshift analysis. For any stable model, the value of the surface redshift lies within 2 [47–49]. We found that our model is stable under the surface redshift 1.714, as can be observed from Fig. 5, whereas in Fig. 6, the feature of the surface mass is exhibited. However, one can note that the surface redshift computation, in order to check the stability of gravastar model, is basically a very cursory check at best. A more proper evaluation of the stability would require a linearized stability analysis or a dynamical analysis, the latter presumably performed numerically. This aspect is beyond the scope of the present investigation and can be considered in the future project.

Now, the question arises regarding the possible existence and detection of the gravastar in our present study. Though there are no direct evidences to detect gravastar, but some of the indirect ways have been discussed in literature [57–62]. The idea for possible detection of gravastar was first proposed by Sakai *et al.* [57] through the study of gravastar shadows. Another possible method for the detection of gravastar may be employing gravitational lensing as suggested by Kubo and Sakai [58], where they claimed to have found gravastar microlensing effects of larger maximal luminosity compared to black holes of the same mass. According to Cardoso *et al.* [60,61], the ringdown signal of *GW*150914 [59] detected by interferometric LIGO detectors is most probably generated by objects without event horizon which might be gravastar, though it is yet to be confirmed [62] (in this context, a detailed review on gravastar can be found in Ref. [63]).

As a final comment, we can conclude that in the present paper a successful study was done on gravastar under the braneworld theory of gravity. We obtained a set of physically acceptable and nonsingular solutions of the gravastar, which immediately overcome the problem of the central singularity and the existence of the event horizon of black hole. One can note that this work provides a general solution of the gravastar in the framework of braneworld gravity without admitting conformal motion unlike Banerjee *et al.* [41]. The solution for the exterior metric was found to be Schwarzschild type, whereas Banerjee *et al.* [41] found the solution as Reissner-Nordström type. Analyzing all the results that we obtained, we claim the possible existence of gravastar in braneworld theory as obtained in Einstein's GR.

ACKNOWLEDGMENTS

S. R., B. M., and S. K. T. are thankful to the Inter-University Centre for Astronomy and Astrophysics, Pune, India for providing the Visiting Associateship under which a part of this work was carried out.

[1] S. W. Hawking and G. F. R. Ellis, *The Large Scale Structure of Space-Time* (Cambridge University Press, Cambridge, England, 1973).
[2] S. W. Hawking, Nature (London) **248**, 30 (1974).
[3] N. D. Birrell and P. C. W. Davies, *Quantum Fields in Curved Space* (Cambridge University Press, Cambridge, England, 1982).
[4] P. Mazur and E. Mottola, Report No. LA-UR-01-5067, 2001, arXiv:gr-qc/0109035v5.
[5] P. Mazur and E. Mottola, Proc. Natl. Acad. Sci. U.S.A. **101**, 9545 (2004).
[6] G. Chapline, E. Hohlfield, R. B. Laughlin, and D. I. Santiago, Philos. Mag. B **81**, 235 (2001).
[7] R. B. Laughlin, Int. J. Mod. Phys. A **18**, 831 (2003).
[8] G. Chapline, E. Hohlfield, R. B. Laughlin, and D. I. Santiago, Int. J. Mod. Phys. A **18**, 3587 (2003).
[9] E. B. Gliner, Zh. Eksp. Teor. Fiz. **49**, 542 (1965) [J. Exp. Theor. Phys. **22**, 378 (1966)].
[10] Ya. B. Zeldovich, J. Exp. Theor. Phys. **14**, 11437 (1962).
[11] Y. B. Zeldovich, Mon. Not. R. Astron. Soc. **160**, 1 (1972).
[12] L. Randall and R. Sundrum, Phys. Rev. Lett. **83**, 3370 (1999).
[13] L. Randall and R. Sundrum, Phys. Rev. Lett. **83**, 4690 (1999).
[14] P. Binetruy, C. Deffayet, U. Ellwanger, and D. Langlois, Phys. Lett. B **477**, 285 (2000).
[15] K. I. Maeda and D. Wands, Phys. Rev. D **62**, 124009 (2000).
[16] R. Maartens, Phys. Rev. D **62**, 084023 (2000).
[17] D. Langlois, Phys. Rev. Lett. **86**, 2212 (2001).
[18] C.-M. Chen, T. Harko, and M. K. Mak, Phys. Rev. D **64**, 044013 (2001).
[19] E. Kiritsis, J. Cosmol. Astropart. Phys. 10 (2005) 014.
[20] A. Campos and C. F. Sopuerta, Phys. Rev. D **63**, 104012 (2001).
[21] C. Germani and R. Maartens, Phys. Rev. D **64**, 124010 (2001).
[22] N. Deruelle, arXiv:gr-qc/0111065.
[23] T. Wiseman, Phys. Rev. D **65**, 124007 (2002).
[24] M. Visser and D. L. Wiltshire, Phys. Rev. D **67**, 104004 (2003).
[25] S. Creek, R. Gregory, P. Kanti, and B. Mistry, Classical Quantum Gravity **23**, 6633 (2006).
[26] S. Pal, Phys. Rev. D **74**, 124019 (2006).
[27] N. Dadhich and S. G. Ghosh, Phys. Lett. B **518**, 1 (2001).

[28] M. Bruni, C. Germani, and R. Maartens, Phys. Rev. Lett. **87**, 231302 (2001).
[29] M. Govender and N. Dadhich, Phys. Lett. B **538**, 233 (2002).
[30] T. Wiseman, Classical Quantum Gravity **19**, 3083 (2002).
[31] D. Kramer, H. Stephani, E. Herlt, and M. MacCallum, *Exact Solutions of Einstein's Field Equations* (Cambridge University Press, Cambridge, England, 1980).
[32] T. Shiromizu, K.-I. Maeda, and M. Sasaki, Phys. Rev. D **62**, 024012 (2000).
[33] J. Ovalle, Mod. Phys. Lett. A **23**, 3247 (2008).
[34] J. Ovalle, Int. J. Mod. Phys. D **18**, 837 (2009).
[35] J. Ovalle, arXiv:gr-qc/0909.0531.
[36] J. Ovalle, Mod. Phys. Lett. A **25**, 3323 (2010).
[37] R. Casadio and J. Ovalle, Phys. Lett. B **715**, 251 (2012).
[38] R. Casadio, J. Ovalle, and R. da Rocha, Classical Quantum Gravity **31**, 045016 (2014).
[39] L. Visinelli, N. Bolis, and S. Vagnozzi, Phys. Rev. D **97**, 064039 (2018).
[40] S. Vagnozzi and L. Visinelli, Phys. Rev. D **100**, 024020 (2019).
[41] A. Banerjee, F. Rahaman, S. Islam, and M. Govender, Eur. Phys. J. C **76**, 1 (2016).
[42] S. Ghosh, F. Rahaman, B. K. Guha, and S. Ray, Phys. Lett. B **767**, 380 (2017).
[43] L. B. Castro, M. D. Alloy, and D. P. Menezes, J. Cosmol. Astropart. Phys. 08 (2014) 047.
[44] A. Banerjee, P. H. R. S. Moraes, R. A. C. Correa, and G. Ribeiro, arXiv:gr-qc/1904.10310.
[45] C. Cattoen, T. Faber, and M. Visser, Classical Quantum Gravity **22**, 4189 (2005).
[46] R. Maartens, Living Rev. Relativity **7**, 7 (2004).
[47] H. A. Buchdahl, Phys. Rev. **116**, 1027 (1959).
[48] N. Straumann, *General Relativity and Relativistic Astrophysics* (Springer, Berlin, 1984).
[49] C. G. Böhmer and T. Harko, Classical Quantum Gravity **23**, 6479 (2006).
[50] G. Darmois, *Mémorial des sciences mathématiques, Fascicule XXV* (Gauthier-Villars, Paris, 1927), Chap. V.
[51] W. Israel, Nuovo Cimento B **66**, 1 (1966); Nuovo Cimento B **48**, 463(E) (1967).
[52] C. Lanczos, Ann. Phys. **74**, 518 (1924), https://doi.org/10.1002/andp.19243791403.
[53] M. F. Shamir and M. Ahmad, Phys. Rev. D **97**, 104031 (2018).
[54] A. Das, S. Ghosh, B. K. Guha, S. Das, F. Rahaman, and S. Ray, Phys. Rev. D **95**, 124011 (2017).
[55] U. Debnath, Eur. Phys. J. C **79**, 499 (2019).
[56] U. Debnath, arXiv:gen-ph/1909.01139.
[57] N. Sakai, H. Saida, and T. Tamaki, Phys. Rev. D **90**, 104013 (2014).
[58] T. Kubo and N. Sakai, Phys. Rev. D **93**, 084051 (2016).
[59] B. P. Abbott *et al.* (LIGO and Virgo Scientific Collaborations), Phys. Rev. Lett. **116**, 061102 (2016).
[60] V. Cardoso, E. Franzin, and P. Pani, Phys. Rev. Lett. **116**, 171101 (2016).
[61] V. Cardoso, E. Franzin, and P. Pani, Phys. Rev. Lett. **117**, 089902(E) (2016).
[62] C. Chirenti and L. Rezzolla, Phys. Rev. D **94**, 084016 (2016).
[63] S. Ray, R. Sengupta, and H. Nimesh, Int. J. Mod. Phys. D **29**, 2030004 (2020).